Carbonate stability in the reduced lower mantle

Susannah Dorfman, James Badro, Farhang Nabiei, Vitali Prakapenka, Marco Cantoni, Philippe Gillet

Carbonate stability in the reduced lower mantle

Authors: Susannah M. Dorfman[1,2]*, James Badro[3,1] , Farhang Nabiei[1], Vitali B. Prakapenka[4], Marco Cantoni[5], Philippe Gillet[1]

Affiliations:

[1]Earth and Planetary Science Laboratory, Ecole polytechnique fédérale de Lausanne, Station 3, CH-1015 Lausanne, Switzerland.

[2]Department of Earth and Environmental Sciences, Michigan State University, East Lansing, MI, 48824, USA.

[3]Institut de Physique du Globe de Paris, Sorbonne Paris Cité, UMR CNRS 7154, 75005 Paris, France.

[4]Center for Advanced Radiation Sources, University of Chicago, Argonne, IL 60439, USA.

[5]Centre Interdisciplinaire de Microscopie Electronique, Ecole polytechnique fédérale de Lausanne, Station 12, 1015 Lausanne, Switzerland.

*Correspondence to: dorfman3@msu.edu

Abstract

Carbonate minerals are important hosts of carbon in the crust and mantle with a key role in the transport and storage of carbon in Earth's deep interior over the history of the planet. Whether subducted carbonates efficiently melt and break down due to interactions with reduced phases or are preserved to great depths and ultimately reach the core-mantle boundary remains controversial. In this study, experiments in the laser-heated diamond anvil cell (LHDAC) on layered samples of dolomite $(Mg,Ca)CO_3$ and iron at pressure and temperature conditions reaching those of the deep lower mantle show that carbon-iron redox interactions destabilize the $MgCO_3$ component, producing a mixture of diamond, Fe_7C_3, and (Mg,Fe)O. However, $CaCO_3$ is preserved, supporting its relative stability in carbonate-rich lithologies under reducing lower mantle conditions. These results constrain the thermodynamic stability of redox-driven breakdown of carbonates and demonstrate progress towards multiphase mantle petrology in the LHDAC at conditions of the lowermost mantle.

1. Introduction

Carbonates are the major minerals responsible for transportation of carbon from the Earth's surface to its deep interior. Their behavior at depth is critical to the storage capacity and fluxes of the geologic carbon cycle. Recent estimates of the flux of carbon trapped in carbonate minerals that reach the deep Earth range from 0.0001 to 52 megatons annually (Dasgupta and Hirschmann, 2010; Kelemen and Manning, 2015). The uncertainty in this range hinges on poor constraints on the budget of carbon retained by subducting slabs. Transport of carbon to at least transition zone depths is demonstrated by carbonate inclusions in diamonds (e.g. Brenker et al., 2007; Wang et al., 1996), but whether any carbonates remain in the lower mantle is controversial. Most subducted carbon is expected to melt and/or break down and return to

Earth's surface via volcanism (Dasgupta and Hirschmann, 2010; Kelemen and Manning, 2015; Thomson et al., 2016). However, relatively oxidizing conditions, low temperatures, and resulting slow kinetics within subducting slabs may result in transportation of carbonates magnesite, siderite, calcite, and their solid solutions to great depths (Martirosyan et al., 2016). Subducted carbonates in slabs that reach the base of the lower mantle will undergo multiple phase transitions and encounter reducing conditions, to be finally buffered by metallic iron at or near the CMB.

Carbon provides key constraints on the chemical evolution of the deep Earth through its role as a proxy for mantle redox conditions, as its speciation is largely governed by oxygen fugacity, or f_{O2} (Frost and McCammon, 2008). Evidence of deep mantle chemistry (Walter et al., 2011) and redox state (Ryabchikov and Kaminsky, 2013; Smith et al., 2016) in local environments of diamond formation can likely be inferred from diamond inclusions. Diamonds and their inclusions indicate widely varying local f_{O2} (Brenker et al., 2007; Walter et al., 2011; Ryabchikov and Kaminsky, 2013; Smith et al., 2016; Kaminsky, 2012), though f_{O2} is expected to generally decrease with mantle depth (Frost and McCammon, 2008; Rohrbach and Schmidt, 2011). Both isotopic evidence (e.g. Harte, 2010; Tappert et al., 2005) and carbonate inclusions in diamonds (e.g. Wang et al., 1996) suggest that diamonds are (at least in part) formed by reduction of subducted carbonate minerals or carbonate melts. Reduction of carbonates to diamond takes place by interactions with mantle silicates (Pal'yanov et al., 2002; Stagno et al., 2011, 2013, 2015) or metal (Arima et al., 2002; Siebert et al., 2005; Rouquette et al., 2008; Pal'yanov et al., 2013). These redox reactions contribute to the barrier to carbonate transport to the deep Earth (Rohrbach and Schmidt, 2011; Thomson et al., 2016). The key to determining the

amount of oxidized carbon in the deep Earth is the dependence of both the thermodynamics and the kinetics of redox reactions in carbonates on temperature, pressure, and f_{O2}.

Petrologic observations, experiments and computational studies on stability and breakdown kinetics of carbonates have determined that magnesite is the most stable carbonate phase throughout most of the mantle (e.g. Dasgupta and Hirschmann, 2010; Rohrbach and Schmidt, 2011), but calcite and siderite polymorphs have also attracted interest. Relative to aragonite (Spivak et al., 2011) or siderite (Tao et al., 2013), magnesite is more likely to subduct to the deep mantle due to its higher melting temperature (Isshiki et al., 2004; Katsura and Ito, 1990; Martinez et al., 1998; Solopova et al., 2014). Melting experiments on carbonated peridotite (Dasgupta and Hirschmann, 2010; Ghosh et al., 2014; Rohrbach and Schmidt, 2011) and eclogite (Thomson et al., 2016) systems confirm that calcium and iron carbonate components are more likely to enter a melt phase than magnesium carbonate in silicate lithologies. At sub-solidus temperatures, $MgCO_3$ is also favored in carbonate-silicate mixtures by the reaction $CaCO_3 + MgSiO_3 \rightarrow MgCO_3 + CaSiO_3$ at lower-mantle pressures up to 80 GPa (Biellmann et al., 1993; Seto et al., 2008). Due to its broad solid solution with siderite (Lin et al., 2012; Liu et al., 2015), magnesite in the mantle will host iron. An (Mg,Fe)-carbonate in the lowermost mantle may have mixed redox state and coexist with diamond (Boulard et al., 2012). However, both $(Mg,Fe)CO_3$ (Brenker et al., 2007; Kaminsky et al., 2016; Phillips and Harris, 1995; Ryabchikov and Kaminsky, 2013) and $CaCO_3$ (Brenker et al., 2007; Meyer and McCallum, 1986) have been observed in inclusions in diamonds, including ultra-deep diamonds from the transition zone or possibly the lower mantle (Brenker et al., 2007). These inclusions demonstrate that both $(Mg,Fe)CO_3$ and $CaCO_3$ may be preserved by kinetic effects within carbonate-rich sediment in cold subducting slabs, consistent with slow breakdown kinetics observed in experiments at

transition zone conditions (Martirosyan et al., 2016). The relative stability of (Mg,Fe)CO_3 and $CaCO_3$ may also change at depth due to polymorphism. If (Mg,Fe)CO_3 or $CaCO_3$ reaches the base of the lower mantle, density functional theory calculations (Oganov et al., 2008; Pickard and Needs, 2015) and experiments (Boulard et al., 2011; Ono et al., 2007) suggest these carbonates will transform to tetrahedrally-coordinated structures. If the transition in $CaCO_3$ occurs at a shallower depth than the analogous transition in $MgCO_3$, as predicted by Pickard and Needs (2015), $CaCO_3$ would be the denser and more energetically-favored carbonate in the deep lower mantle.

This study examines a Mg-Fe-Ca carbonate system in the petrologic context of a subducted carbonate assemblage in contact with metallic iron. Metallic iron may be present at the percent level throughout the mantle (Frost et al., 2004), and the outer core provides an unlimited reservoir of iron. Subducted carbonates may contact reduced core-mantle mixing regions if they reach depths within ~10s km from the base of the mantle (Frost and McCammon, 2008; Otsuka and Karato, 2012). Previous studies of carbonates at lower mantle pressures have investigated mineralogical stability of single phases as a function of pressure and temperature alone (Isshiki et al., 2004; Solopova et al., 2014; Boulard et al., 2011; Ono et al., 2005), or used mixtures of carbonates and silicates which complicate textural analysis of run products (Biellmann et al., 1993; Thomson et al., 2014). In contrast, we examine reaction interfaces between multiple carbonates and iron; similar previous studies have been limited to transition zone conditions (Martirosyan et al., 2016; Pal'yanov et al., 2013). We determine the relative stability and metastability of Mg-, Fe-, and Ca-carbonates as host phases for oxidized carbon storage in the lower mantle.

2. Methods

To bring experimental petrology of carbonates to the Mbar pressures and 1000s K temperatures of the core-mantle boundary, experiments must be miniaturized: sample geometry must be controlled within the ~50x50x10-micron chamber of the laser-heated diamond anvil cell, and analysis must be performed with ~100-nm-scale spatial resolution of typical grain sizes of run products. Dolomite, a major constituent of subducted marble, provides a unique advantage as a starting material as it has a mixed Mg-Fe-Ca carbonate composition homogeneous to <nm scale. Natural dolomite crystals with composition determined to be $(Mg_{0.38}Ca_{0.59}Fe_{0.03})CO_3$ by X-ray fluorescence spectroscopy and structure confirmed by X-ray diffraction were used as starting materials. Single dolomite crystals were polished to ~10-micron thickness and dried in a 120°C oven overnight before loading. 3-micron thick 99.85% iron foil was machined into discs with a ps-pulsed 532-nm laser or cut with a razor blade. Iron foils were loaded sandwiched between dolomite crystals in symmetric diamond anvil cells. No other pressure standard or medium was loaded in order to prevent reactions with other components and contamination of the chemical system. Sample sandwiches were loaded within chambers cut in Re gaskets in diamond anvil cells. Diamond anvils with flat culets of 200 micron diameter or beveled culets of 150 micron diameter were chosen to generate pressures corresponding to the lower mantle.

Samples were compressed to pressures of 51, 66, 77, and 113 GPa, as determined by the equation of state of the iron foil (Mao et al., 1990) before laser heating (Table 1). Pressures were not measured during heating due to chemical reaction of the iron foil with the dolomite, but were likely ~7-10 GPa higher than those reported here due to thermal pressure. Laser heating was performed with *in situ* X-ray diffraction at the GSECARS sector of the Advanced Photon Source

129 (Prakapenka et al., 2008). The laser spot was focused to a diameter of ~10 microns with a flat-
130 top beam shape. Each sample was heated for 10-20 min at 1800-2500 K.
131 After recovery to ambient conditions, each heated spot was sectioned using a Zeiss NVision
132 40 dual-beam scanning electron microscope and focused Ga^+ ion beam (Centre Interdisciplinaire
133 Microscopie de Electronique (CIME), EPFL). Each sample was coated with 15 nm Au to reduce
134 charging in the scanning electron microscope. To protect the samples from damage by the Ga^+
135 ion beam, an additional ~1-2 micron thick layer of Pt or C was deposited across the centers of
136 heated spots. Thin sections of each heated spot were extracted and polished to electron
137 transparency (~100 nm thickness).
138 Imaging of recovered thin sections was performed with scanning transmission election
139 microscopy (S/TEM) and energy-dispersive X-ray spectroscopy (EDX) in a FEI Tecnai Osiris
140 analytical TEM (CIME, EPFL). Accelerating voltage for these measurements was 200 kV. The
141 Osiris TEM is equipped with four wide-solid-angle detectors for high-speed chemical
142 measurements by EDX spectroscopy. EDX maps were scanned over 1024x1024 pixel areas with
143 pixel dwell time of 50 microseconds. Typical count rates were ~40,000-50,000 counts per
144 second. Chemical mapping prevents migration of elements due to damage by the electron beam.
145 Uncertainties in compositions were determined from standard deviations of EDX measurements
146 obtained from selected regions within multiple grains.

147 **3. Results**

148 Laser-heating dolomite-iron sandwiches from both sides produces a lens-shaped heated
149 zone (Figure 1), as predicted by models (Kiefer and Duffy, 2005; Rainey et al., 2013) and
150 measurements (Campbell, 2008) of thermal diffusion in the diamond anvil cell. Laser absorption

151 and diffraction indicate that the sample reaches a steady state within a few minutes. The hottest
152 region of the sample is the laser-absorbing central iron layer. The insulating dolomite layers
153 experience both axial and radial temperature gradients, with highest temperatures at the contacts
154 with the iron foil and lowest temperatures at the diamond anvil surface. High-resolution TEM
155 inspection of recovered thin sections indicates that grain sizes decrease away from the surface of
156 the iron foil, consistent with this thermal gradient (Figure 1). At the cool upper and lower edges
157 of the heated spot, ribbons of magnesium and calcium carbonate exsolve from the dolomite
158 (Figure 2), as has been observed at lower pressures (Sato and Katsura, 2001; Shirasaka et al.,
159 2002).

160 Both EDX analysis of recovered thin sections in the TEM (Figure 3) and diffraction
161 patterns obtained during and after sub-solidus laser heating (Figure 4b) show that the metallic
162 iron at the sample center reacts completely with the dolomite to generate a mixture of FeO and
163 Fe_7C_3. The iron layer thus exhibits oxidation which must be compensated by reduction of the
164 carbonate. Within the carbonate layer near the hot interface with the iron foil, three phases are
165 found in all samples: diamond, Mg-bearing ferropericlase, and $CaCO_3$ (Figure 3). The diffusion
166 of iron from the sample center propagates breakdown of the magnesium carbonate to diamond
167 and ferropericlase. Due to diffusion, this ferropericlase has much more MgO than the FeO at the
168 sample center (Figures 5-6). Unlike $MgCO_3$, $CaCO_3$ exsolves from the dolomite but is never
169 observed to break down. EDX composition analysis confirms that the $CaCO_3$ phase retains both
170 O and C within measurement error and there is no evidence for measurable Ca in any other phase
171 (Figure 5). At the pressures examined here, the stable polymorph of $CaCO_3$ is the post-aragonite
172 phase (Ono et al., 2005). Post-aragonite-type $CaCO_3$ is observed in diffraction patterns after
173 heating (Figure 4b), along with unreacted dolomite. These experiments show that a carbonate-

174 rich rock such as subducted marble subjected to reducing conditions in contact with metallic
175 iron, post-aragonite-type $CaCO_3$ is a more stable form of carbonate than $MgCO_3$ throughout the
176 lower mantle pressure range.

177 **4. Discussion**

178 The mixture of (Mg,Fe)O, diamond, Fe_7C_3 and $CaCO_3$ is produced by redox coupling
179 between the iron and carbon and breakdown of the $MgCO_3$ component. The following reactions
180 explain these observations:

181 $MgCO_3 + 2Fe \rightarrow C + MgO + 2FeO$

182 $3MgCO_3 + 13Fe \rightarrow Fe_7C_3 + 3MgO + 6FeO$

183 In the center of the sample, the system is saturated in iron, leading to a mixture
184 dominated by Fe_7C_3 and FeO. In the region where the carbonate breaks down, the carbon/iron
185 ratio is higher, and reduced carbon is found in diamonds rather than carbides. The breakdown of
186 $MgCO_3$ is favorable in all heated regions in the presence of iron. The stable host phase for
187 carbon is controlled by the Fe/$MgCO_3$ ratio of reactants. Recent studies have largely focused on
188 (Mg,Fe)CO_3 as a host phase for oxidized carbon in the deep Earth, as the melting point of
189 magnesite or ferromagnesite is higher than that of $CaCO_3$ in the transition zone. However,
190 (Mg,Fe)CO_3 is much more susceptible to redox breakdown than $CaCO_3$.

191 Redox breakdown will promote diamond formation from (Mg,Fe)CO_3 in carbonated
192 eclogite and peridotite. This study and others have shown that diamonds nucleate and grow
193 directly from carbonates at subsolidus, reducing conditions, and inclusion-bearing diamonds
194 used as evidence that carbonates are stable to great depths in the mantle record incomplete redox
195 breakdown (e.g. Wang et al., 1996). Reducing agents relevant to carbonate stability at different

196 stages of Earth's chemical evolution include graphite (Pal'yanov et al., 1999), H_2 (Pal'yanov et
197 al., 2002), Si metal (Siebert et al., 2005), and Fe metal. In a mixture of carbonate and Fe-Si alloy,
198 Si and C were oxidized, producing a mixture in which diamonds coexist with metallic iron
199 (Siebert et al., 2005). Other studies have suggested either that pure iron and pure carbon should
200 not coexist in equilibrium (Rouquette et al., 2008; Scott et al., 2001) or that iron carbides and
201 diamond compete as hosts of reduced carbon (Iizuka et al., 1996). In this study, metallic iron
202 reacts completely to carbide and oxide, indicating that the system is oversaturated in carbon.
203 Because the mantle has been suggested to be a highly reducing environment, saturated in
204 metallic iron (Frost et al., 2004; Frost and McCammon, 2008; Rohrbach et al., 2007; Rohrbach
205 and Schmidt, 2011), carbonate in this system will be susceptible to redox breakdown at
206 subsolidus temperatures. Reduction of subducted carbonates by interaction with metallic iron
207 was previously explored at relatively modest depths (Martin and Hammouda, 2011; Martirosyan
208 et al., 2015a, 2015b; Stagno et al., 2011). Most previous studies were conducted at pressures
209 reaching ~6 GPa (Martin and Hammouda, 2011; Martirosyan et al., 2015a, 2015b), too low to
210 model the depths at which metallic iron becomes available to react with subducted carbonate.
211 Metallic iron may also be present in the lower mantle due to charge disproportionation in
212 silicates (Frost et al., 2004; Rohrbach et al., 2007), mixing at the CMB (Knittle and Jeanloz,
213 1989; Otsuka and Karato, 2012), or residue of magma ocean solidification (Zhang et al., 2016).
214 Recently, iron-magnesite mixtures were examined at 16-45 GPa and 1500-1700 °C,
215 corresponding to transition zone to lower mantle depths (Stagno et al., 2011). At these
216 conditions, diamonds are observed to coexist with magnesite, ferropericlase and carbon-free
217 iron-iridium alloy. The Ir alloy was used to determine that f_{O2} was ~3 log units above the iron-
218 wüstite buffer. The breakdown of magnesite observed here may imply lower f_{O2} conditions,

perhaps due to the sample environment in the diamond anvil cell or higher pressures. For subducted marble or carbonated silicate lithologies that reach a reduced zone near the core-mantle boundary, $(Mg,Fe)CO_3$ cannot be preserved.

Spin transitions in ferromagnesite have recently been studied for their potential to affect carbonate stability (Lin et al., 2012; Liu et al., 2015). The spin transition results in a ~8% unit cell volume collapse for $(Mg_{0.35}Fe_{0.65})CO_3$ (Lin et al., 2012) and would thus be expected to have a significant effect on phase equilibria. As the minimum pressure examined in these experiments is above the spin transition pressure, we are unable to evaluate whether the spin transition is related to the observed breakdown of $(Mg,Fe)CO_3$. The susceptibility of $(Mg,Fe)CO_3$ to disproportionation at low f_{O2} suggests that low-spin iron-bearing carbonates are unlikely to be stable in Earth's mantle.

$CaCO_3$ is less sensitive than $(Mg,Fe)CO_3$ to redox breakdown, but melting, reaction with silicates, and buoyancy remain challenging barriers to its transport to the deep mantle. Although the melting point of $CaCO_3$ (Bayarjargal et al., 2010; Thomson et al., 2014) is well above a 1600 K adiabatic geotherm (Brown and Shankland, 1981), the eutectic melting point for carbonate mixtures is substantially lower and comparable to the geotherm (Thomson et al., 2014). Eutectic melting has been argued to effectively block carbonate transport to the lower mantle (Thomson et al., 2016). However, no evidence is observed for melting of the dolomite carbonate in this work. Moreover, geotherms both for the average mantle (e.g. Brown and Shankland, 1981; Andrault et al., 2011; Nomura et al., 2014) and subducting slabs (e.g. Andrault et al., 2014) remain highly uncertain. The key question is whether, for realistic subducted carbonates, the melting point of the mixture is high enough relative to the temperature in the slab to prevent diamond formation. With temperature uncertainties of at least 100s K, in addition to potential

kinetic effects on the efficiency of carbonate reduction and melting (Martirosyan et al., 2016), preservation of carbonates in the lower mantle cannot yet be ruled out. $CaCO_3$ is also expected to be destabilized in the mantle by reaction with $(Mg,Fe)SiO_3$ in peridotite or eclogite to produce $CaSiO_3$ and $(Mg,Fe)CO_3$ (Biellmann et al., 1993; Seto et al., 2008). This reaction suggests $CaCO_3$ is most likely to be preserved in silicate-poor, dolomite-rich marble entrained with subducting slabs. Because metasediment is likely to be as much as ~5-15% less dense than surrounding peridotite, ~100 m packages of marble would likely rise to the surface through diapirism (Kelemen and Manning, 2015). Transport of $CaCO_3$ to the deep mantle would require carbonate to reside in layers or regions thin enough to be entrained with the cold slab, but thick enough that slow diffusion blocks reaction of carbonate with silicates.

Observations in this and other experimental studies challenge interpretation of oxide inclusions in identified in diamonds. While traditionally (Mg,Fe)O inclusions have been considered to be a smoking gun for formation in the Earth's lower mantle, as a leftover from the breakdown of Mg_2SiO_4 to lower mantle bridgmanite (Kaminsky, 2012), carbonate disproportionation is another possible mechanism for oxide formation (Tappert et al., 2005; Thomson et al., 2016). Direct observation of lower mantle silicates of appropriate compositions is necessary to confirm ultra-deep diamond origin.

5. Conclusions

Magnesite-siderite is not a likely host phase for carbonate in reduced regions of the deep lower mantle, but post-aragonite-type $CaCO_3$ may be stable in carbonate-rich lithologies. While $CaCO_3$ undergoes more pressure-induced polymorphic transitions than $(Mg,Fe)CO_3$ in the deep mantle and may be more likely to react with lower mantle silicates, relative to $(Mg,Fe)CO_3$ it is less likely to participate in redox reactions. A low f_{O2} environment in the lower mantle (Frost and

McCammon, 2008; Rohrbach and Schmidt, 2011) will promote breakdown of ferromagnesite but $CaCO_3$ will remain stable to pressure, temperature and redox conditions near the base of the lower mantle if isolated from silicates. A carbonate-rich heterogeneity near the base of the mantle could be a high-pressure marble, with $CaCO_3$ associated with diamonds formed by breakdown of $MgCO_3$.

Diamond-bearing marble in the lower mantle is not likely to be directly observable by seismic tomography, but could impact observations of heterogeneous redox conditions at depth due to mantle convection and subduction and/or signatures of Earth's chemical evolution. Heterogeneous oxygen fugacity at depth is evident in diamond inclusions (Brenker et al., 2007; Walter et al., 2011; Ryabchikov and Kaminsky, 2013; Smith et al., 2016; Kaminsky, 2012) as well as chemical variation in both mid-ocean ridge basalts due to relative contributions of depleted and primitive mantle sources (Cottrell and Kelley, 2013) and ocean island basalts potentially sourced from the core-mantle boundary (White, 2010). The interpretation of available redox proxies for the deep mantle over deep time, particularly presence of carbonate (e.g. Brenker et al., 2007) and speciation of iron (Frost and McCammon, 2008), must be evaluated in the light of the multivariable dependence of stability of $MgCO_3$ and $CaCO_3$ on temperature, bulk composition of the phase assemblage and f_{O2}.

Acknowledgments:

The authors acknowledge M. Hirschmann for thoughtful comments that improved this manuscript. We thank A. Magrez for assistance with X-ray diffraction and X-ray fluorescence characterization of the starting material. F. Bobard, D. Alexander and E. Oveisi provided training and advice for focused ion beam and transmission electron microscopy. S. M. Dorfman acknowledges the Marie Heim-Vögtlin program of the Swiss National Science Foundation for financial support through project PMPDP2_151256. J. Badro acknowledges the financial support of the Sloan Foundation's Deep Carbon Observatory and UnivEarthS Labex program at Sorbonne Paris Cité (ANR-10-LABX-0023 and ANR-11-IDEX-0005-02). GeoSoilEnviroCARS

291 is supported by the National Science Foundation - Earth Sciences (EAR-0622171), Department
292 of Energy - Geosciences (DE-FG02-94ER14466) and the State of Illinois.

293 Data reported in this paper are available by request from S. M. Dorfman at
294 dorfman3@msu.edu.

295
296

References:

Andrault, D., Bolfan-Casanova, N., Nigro, G.L., Bouhifd, M.A., Garbarino, G., Mezouar, M., 2011. Solidus and liquidus profiles of chondritic mantle: Implication for melting of the Earth across its history. Earth Planet. Sci. Lett. 304, 251–259. https://doi.org/10.1016/j.epsl.2011.02.006

Andrault, D., Pesce, G., Bouhifd, M.A., Bolfan-Casanova, N., Hénot, J.-M., Mezouar, M., 2014. Melting of subducted basalt at the core-mantle boundary. Science 344, 892–895. https://doi.org/10.1126/science.1250466

Arima, M., Kozai, Y., Akaishi, M., 2002. Diamond nucleation and growth by reduction of carbonate melts under high-pressure and high-temperature conditions. Geology 30, 691–694. https://doi.org/10.1130/0091-7613(2002)030<0691:DNAGBR>2.0.CO;2

Bayarjargal, L., Shumilova, T.G., Friedrich, A., Winkler, B., 2010. Diamond formation from $CaCO_3$ at high pressure and temperature. Eur. J. Mineral. 22, 29–34. https://doi.org/10.1127/0935-1221/2010/0021-1986

Biellmann, C., Gillet, P., Guyot, F., Peyronneau, J., Reynard, B., 1993. Experimental evidence for carbonate stability in the Earth's lower mantle. Earth Planet. Sci. Lett. 118, 31–41. https://doi.org/10.1016/0012-821X(93)90157-5

Boulard, E., Gloter, A., Corgne, A., Antonangeli, D., Auzende, A.-L., Perrillat, J.-P., Guyot, F., Fiquet, G., 2011. New host for carbon in the deep Earth. PNAS 108, 5184–5187. https://doi.org/10.1073/pnas.1016934108

Boulard, E., Menguy, N., Auzende, A.L., Benzerara, K., Bureau, H., Antonangeli, D., Corgne, A., Morard, G., Siebert, J., Perrillat, J.P., Guyot, F., Fiquet, G., 2012. Experimental investigation of the stability of Fe-rich carbonates in the lower mantle. J. Geophys. Res. 117, B02208. https://doi.org/10.1029/2011JB008733

Brenker, F.E., Vollmer, C., Vincze, L., Vekemans, B., Szymanski, A., Janssens, K., Szaloki, I., Nasdala, L., Joswig, W., Kaminsky, F., 2007. Carbonates from the lower part of transition zone or even the lower mantle. Earth Planet. Sci. Lett. 260, 1–9. https://doi.org/10.1016/j.epsl.2007.02.038

Brown, J.M., Shankland, T.J., 1981. Thermodynamic parameters in the Earth as determined from seismic profiles. Geophys. J. Int. 66, 579–596. https://doi.org/10.1111/j.1365-246X.1981.tb04891.x

Campbell, A.J., 2008. Measurement of temperature distributions across laser heated samples by multispectral imaging radiometry. Rev. Sci. Instrum. 79, 015108. https://doi.org/10.1063/1.2827513

Cottrell, E., Kelley, K.A., 2013. Redox Heterogeneity in Mid-Ocean Ridge Basalts as a Function of Mantle Source. Science 340, 1314–1317. https://doi.org/10.1126/science.1233299

Dasgupta, R., Hirschmann, M.M., 2010. The deep carbon cycle and melting in Earth's interior. Earth Planet. Sci. Lett. 298, 1–13. https://doi.org/10.1016/j.epsl.2010.06.039

Fei, Y., Zhang, L., Corgne, A., Watson, H., Ricolleau, A., Meng, Y., Prakapenka, V., 2007. Spin transition and equations of state of (Mg, Fe)O solid solutions. Geophys. Res. Lett. 34, L17307.

Fischer, R.A., Campbell, A.J., Shofner, G.A., Lord, O.T., Dera, P., Prakapenka, V.B., 2011. Equation of state and phase diagram of FeO. Earth Planet. Sci. Lett. 304, 496–502. https://doi.org/10.1016/j.epsl.2011.02.025

Frost, D.J., Liebske, C., Langenhorst, F., McCammon, C.A., Trønnes, R.G., Rubie, D.C., 2004. Experimental evidence for the existence of iron-rich metal in the Earth's lower mantle. Nature 428, 409–412. https://doi.org/10.1038/nature02413

Frost, D.J., McCammon, C.A., 2008. The redox state of Earth's mantle. Annu. Rev. Earth Planet. Sci. 36, 389–420. https://doi.org/10.1146/annurev.earth.36.031207.124322

Ghosh, S., Litasov, K., Ohtani, E., 2014. Phase relations and melting of carbonated peridotite between 10 and 20 GPa: a proxy for alkali- and CO2-rich silicate melts in the deep mantle. Contrib Mineral Petrol 167, 964. https://doi.org/10.1007/s00410-014-0964-z

Harte, B., 2010. Diamond formation in the deep mantle: the record of mineral inclusions and their distribution in relation to mantle dehydration zones. Mineral. Mag. 74, 189–215. https://doi.org/10.1180/minmag.2010.074.2.189

Iizuka, M., Ikawa, H., Fukunaga, O., 1996. Nucleation and growth of diamond using Ni-Ti, Ni-Nb and Fe-B alloy as solvents. Diamond and Related Materials 5, 38–42. https://doi.org/10.1016/0925-9635(95)00329-0

Isshiki, M., Irifune, T., Hirose, K., Ono, S., Ohishi, Y., Watanuki, T., Nishibori, E., Takata, M., Sakata, M., 2004. Stability of magnesite and its high-pressure form in the lowermost mantle. Nature 427, 60–63. https://doi.org/10.1038/nature02181

Kaminsky, F., 2012. Mineralogy of the lower mantle: A review of "super-deep" mineral inclusions in diamond. Earth-Sci. Rev. 110, 127–147. https://doi.org/10.1016/j.earscirev.2011.10.005

Kaminsky, F.V., Ryabchikov, I.D., Wirth, R., 2016. A primary natrocarbonatitic association in the Deep Earth. Miner Petrol 110, 387–398. https://doi.org/10.1007/s00710-015-0368-4

Katsura, T., Ito, E., 1990. Melting and subsolidus phase relations in the $MgSiO_3$-$MgCO_3$ system at high pressures: implications to evolution of the Earth's atmosphere. Earth Planet. Sci. Lett. 99, 110–117. https://doi.org/10.1016/0012-821X(90)90074-8

Kelemen, P.B., Manning, C.E., 2015. Reevaluating carbon fluxes in subduction zones, what goes down, mostly comes up. PNAS 112, E3997–E4006. https://doi.org/10.1073/pnas.1507889112

Kiefer, B., Duffy, T.S., 2005. Finite element simulations of the laser-heated diamond-anvil cell. J. Appl. Phys. 97, 114902. https://doi.org/10.1063/1.1906292

Knittle, E., Jeanloz, R., 1989. Simulating the core-mantle boundary: An experimental study of high-pressure reactions between silicates and liquid iron. Geophys. Res. Lett. 16, 609–612. https://doi.org/198910.1029/GL016i007p00609

Lin, J.-F., Liu, J., Jacobs, C., Prakapenka, V.B., 2012. Vibrational and elastic properties of ferromagnesite across the electronic spin-pairing transition of iron. Am. Mineral. 97, 583–591. https://doi.org/10.2138/am.2012.3961

Liu, J., Lin, J.-F., Prakapenka, V.B., 2015. High-Pressure Orthorhombic Ferromagnesite as a Potential Deep-Mantle Carbon Carrier. Sci. Rep. 5. https://doi.org/10.1038/srep07640

Mao, H.K., Wu, Y., Chen, L.C., Shu, J.F., Jephcoat, A.P., 1990. Static Compression of Iron to 300 GPa and Fe0.8Ni0.2 Alloy to 260 GPa: Implications for Composition of the Core. J. Geophys. Res. 95, 21737–21742. https://doi.org/199010.1029/JB095iB13p21737

Martin, A.M., Hammouda, T., 2011. Role of iron and reducing conditions on the stability of dolomite + coesite between 4.25 and 6 GPa – a potential mechanism for diamond formation during subduction. Eur J Mineral 23, 5–16. https://doi.org/10.1127/0935-1221/2010/0022-2067

386 Martinez, I., Chamorro Peréz, E.M., Matas, J., Gillet, P., Vidal, G., 1998. Experimental
387 investigation of silicate-carbonate system at high pressure and high temperature. J.
388 Geophys. Res. 103, 5143–5163. https://doi.org/10.1029/97JB03401
389 Martirosyan, N.S., Litasov, K.D., Shatskiy, A., Ohtani, E., 2015a. The reactions between iron
390 and magnesite at 6 GPa and 1273–1873 K: Implication to reduction of subducted
391 carbonate in the deep mantle. J. Miner. Petrol. Sci. 110, 49–59.
392 https://doi.org/10.2465/jmps.141003a
393 Martirosyan, N.S., Litasov, K.D., Shatskiy, A.F., Ohtani, E., 2015b. Reactions of iron with
394 calcium carbonate at 6 GPa and 1273–1873 K: implications for carbonate reduction in the
395 deep mantle. Russ. Geol. Geophys. 56, 1322–1331.
396 https://doi.org/10.1016/j.rgg.2015.08.008
397 Martirosyan, N.S., Yoshino, T., Shatskiy, A., Chanyshev, A.D., Litasov, K.D., 2016. The
398 $CaCO_3$–Fe interaction: Kinetic approach for carbonate subduction to the deep Earth's
399 mantle. Physics of the Earth and Planetary Interiors 259, 1–9.
400 https://doi.org/10.1016/j.pepi.2016.08.008
401 Meyer, H.O.A., McCallum, M.E., 1986. Mineral Inclusions in Diamonds from the Sloan
402 Kimberlites, Colorado. J. Geol. 94, 600–612. https://doi.org/10.1086/629062
403 Nomura, R., Hirose, K., Uesugi, K., Ohishi, Y., Tsuchiyama, A., Miyake, A., Ueno, Y., 2014.
404 Low Core-Mantle Boundary Temperature Inferred from the Solidus of Pyrolite. Science
405 343, 522–525. https://doi.org/10.1126/science.1248186
406 Oganov, A.R., Ono, S., Ma, Y., Glass, C.W., Garcia, A., 2008. Novel high-pressure structures of
407 $MgCO_3$, $CaCO_3$ and CO_2 and their role in Earth's lower mantle. Earth Planet. Sci. Lett.
408 273, 38–47. https://doi.org/10.1016/j.epsl.2008.06.005
409 Ono, S., Kikegawa, T., Ohishi, Y., 2007. High-pressure transition of $CaCO_3$. Am. Mineral. 92,
410 1246–1249. https://doi.org/10.2138/am.2007.2649
411 Ono, S., Kikegawa, T., Ohishi, Y., Tsuchiya, J., 2005. Post-aragonite phase transformation in
412 $CaCO_3$ at 40 GPa. Am. Mineral. 90, 667–671. https://doi.org/10.2138/am.2005.1610
413 Otsuka, K., Karato, S., 2012. Deep penetration of molten iron into the mantle caused by a
414 morphological instability. Nature 492, 243–246. https://doi.org/10.1038/nature11663
415 Pal'yanov, Y.N., Bataleva, Y.V., Sokol, A.G., Borzdov, Y.M., Kupriyanov, I.N., Reutsky, V.N.,
416 Sobolev, N.V., 2013. Mantle–slab interaction and redox mechanism of diamond
417 formation. PNAS 201313340. https://doi.org/10.1073/pnas.1313340110
418 Pal'yanov, Y.N., Sokol, A.G., Borzdov, Y.M., Khokhryakov, A.F., Sobolev, N.V., 2002.
419 Diamond formation through carbonate-silicate interaction. Am. Mineral. 87, 1009–1013.
420 Pal'yanov, Y.N., Sokol, A.G., Borzdov, Y.M., Khokhryakov, A.F., Sobolev, N.V., 1999.
421 Diamond formation from mantle carbonate fluids. Nature 400, 417–418.
422 https://doi.org/10.1038/22678
423 Phillips, D., Harris, J.W., 1995. Geothermobarometry of diamond inclusions from the De Beers
424 Pool Mines, Kimberley, South Africa. Sixth International Kimberlite Conference,
425 Novosibirsk, Extended Abstracts 441–443.
426 Pickard, C.J., Needs, R.J., 2015. Structures and stability of calcium and magnesium carbonates at
427 mantle pressures. Phys. Rev. B 91, 104101. https://doi.org/10.1103/PhysRevB.91.104101
428 Prakapenka, V.B., Kubo, A., Kuznetsov, A., Laskin, A., Shkurikhin, O., Dera, P., Rivers, M.L.,
429 Sutton, S.R., 2008. Advanced flat top laser heating system for high pressure research at

GSECARS: application to the melting behavior of germanium. High Pressure Res. 28, 225–235. https://doi.org/10.1080/08957950802050718

Rainey, E.S.G., Hernlund, J.W., Kavner, A., 2013. Temperature distributions in the laser-heated diamond anvil cell from 3-D numerical modeling. J. Appl. Phys. 114, 4905. https://doi.org/10.1063/1.4830274

Rohrbach, A., Ballhaus, C., Golla–Schindler, U., Ulmer, P., Kamenetsky, V.S., Kuzmin, D.V., 2007. Metal saturation in the upper mantle. Nature 449, 456–458. https://doi.org/10.1038/nature06183

Rohrbach, A., Schmidt, M.W., 2011. Redox freezing and melting in the Earth's deep mantle resulting from carbon-iron redox coupling. Nature 472, 209–212. https://doi.org/10.1038/nature09899

Rouquette, J., Dolejš, D., Kantor, I.Y., McCammon, C.A., Frost, D.J., Prakapenka, V.B., Dubrovinsky, L.S., 2008. Iron-carbon interactions at high temperatures and pressures. Appl. Phys. Lett. 92, 121912. https://doi.org/10.1063/1.2892400

Ryabchikov, I.D., Kaminsky, F.V., 2013. Oxygen potential of diamond formation in the lower mantle. Geol. Ore Deposits 55, 1–12. https://doi.org/10.1134/S1075701513010066

Sato, K., Katsura, T., 2001. Experimental investigation on dolomite dissociation into aragonite+magnesite up to 8.5 GPa. Earth Planet. Sci. Lett. 184, 529–534. https://doi.org/10.1016/S0012-821X(00)00346-0

Scott, H.P., Williams, Q., Knittle, E., 2001. Stability and equation of state of Fe_3C to 73 GPa: Implications for carbon in the Earth's core. Geophys. Res. Lett. 28, 1875–1878. https://doi.org/10.1029/2000GL012606

Seto, Y., Hamane, D., Nagai, T., Fujino, K., 2008. Fate of carbonates within oceanic plates subducted to the lower mantle, and a possible mechanism of diamond formation. Phys Chem Minerals 35, 223–229. https://doi.org/10.1007/s00269-008-0215-9

Shirasaka, M., Takahashi, E., Nishihara, Y., Matsukage, K., Kikegawa, T., 2002. In situ X-ray observation of the reaction dolomite = aragonite + magnesite at 900–1300 K. Am. Mineral. 87, 922–930.

Siebert, J., Guyot, F., Malavergne, V., 2005. Diamond formation in metal–carbonate interactions. Earth Planet. Sci. Lett. 229, 205–216. https://doi.org/10.1016/j.epsl.2004.10.036

Smith, E.M., Shirey, S.B., Nestola, F., Bullock, E.S., Wang, J., Richardson, S.H., Wang, W., 2016. Large gem diamonds from metallic liquid in Earth's deep mantle. Science 354, 1403–1405. https://doi.org/10.1126/science.aal1303

Solopova, N.A., Dubrovinsky, L., Spivak, A.V., Litvin, Y.A., Dubrovinskaia, N., 2014. Melting and decomposition of $MgCO_3$ at pressures up to 84 GPa. Phys Chem Minerals 42, 73–81. https://doi.org/10.1007/s00269-014-0701-1

Speziale, S., Zha, C.S., Duffy, T.S., Hemley, R.J., Mao, H., 2001. Quasi-hydrostatic compression of magnesium oxide to 52 GPa- Implications for the pressure-volume-temperature equation of state. J. Geophys. Res. 106, 515–528. https://doi.org/10.1029/2000JB900318

Spivak, A.V., Dubrovinskii, L.S., Litvin, Y.A., 2011. Congruent melting of calcium carbonate in a static experiment at 3500 K and 10–22 GPa: Its role in the genesis of ultradeep diamonds. Dokl. Earth Sc. 439, 1171–1174. https://doi.org/10.1134/S1028334X11080319

Stagno, V., Frost, D.J., McCammon, C.A., Mohseni, H., Fei, Y., 2015. The oxygen fugacity at which graphite or diamond forms from carbonate-bearing melts in eclogitic rocks. Contrib Mineral Petrol 169, 16. https://doi.org/10.1007/s00410-015-1111-1

Stagno, V., Ojwang, D.O., McCammon, C.A., Frost, D.J., 2013. The oxidation state of the mantle and the extraction of carbon from Earth's interior. Nature 493, 84–88. https://doi.org/10.1038/nature11679

Stagno, V., Tange, Y., Miyajima, N., McCammon, C.A., Irifune, T., Frost, D.J., 2011. The stability of magnesite in the transition zone and the lower mantle as function of oxygen fugacity. Geophys. Res. Lett. 38, L19309. https://doi.org/10.1029/2011GL049560

Tao, R., Fei, Y., Zhang, L., 2013. Experimental determination of siderite stability at high pressure. Am. Mineral. 98, 1565–1572. https://doi.org/10.2138/am.2013.4351

Tappert, R., Stachel, T., Harris, J.W., Muehlenbachs, K., Ludwig, T., Brey, G.P., 2005. Subducting oceanic crust: The source of deep diamonds. Geology 33, 565–568. https://doi.org/10.1130/G21637.1

Thomson, A.R., Walter, M.J., Kohn, S.C., Brooker, R.A., 2016. Slab melting as a barrier to deep carbon subduction. Nature 529, 76–79. https://doi.org/10.1038/nature16174

Thomson, A.R., Walter, M.J., Lord, O.T., Kohn, S.C., 2014. Experimental determination of melting in the systems enstatite-magnesite and magnesite-calcite from 15 to 80 GPa. Am. Mineral. 99, 1544–1554. https://doi.org/10.2138/am.2014.4735

Walter, M.J., Kohn, S.C., Araujo, D., Bulanova, G.P., Smith, C.B., Gaillou, E., Wang, J., Steele, A., Shirey, S.B., 2011. Deep Mantle Cycling of Oceanic Crust: Evidence from Diamonds and Their Mineral Inclusions. Science 334, 54–57. https://doi.org/10.1126/science.1209300

Wang, A., Pasteris, J.D., Meyer, H.O.A., Dele-Duboi, M.L., 1996. Magnesite-bearing inclusion assemblage in natural diamond. Earth Planet. Sci. Lett. 141, 293–306. https://doi.org/10.1016/0012-821X(96)00053-2

White, W.M., 2010. Oceanic Island Basalts and Mantle Plumes: The Geochemical Perspective. Annual Review of Earth and Planetary Sciences 38, 133–160. https://doi.org/10.1146/annurev-earth-040809-152450

Zhang, Z., Dorfman, S.M., Labidi, J., Zhang, S., Li, M., Manga, M., Stixrude, L., McDonough, W.F., Williams, Q., 2016. Primordial metallic melt in the deep mantle. Geophys. Res. Lett. 43, 3693–3699. https://doi.org/10.1002/2016GL068560

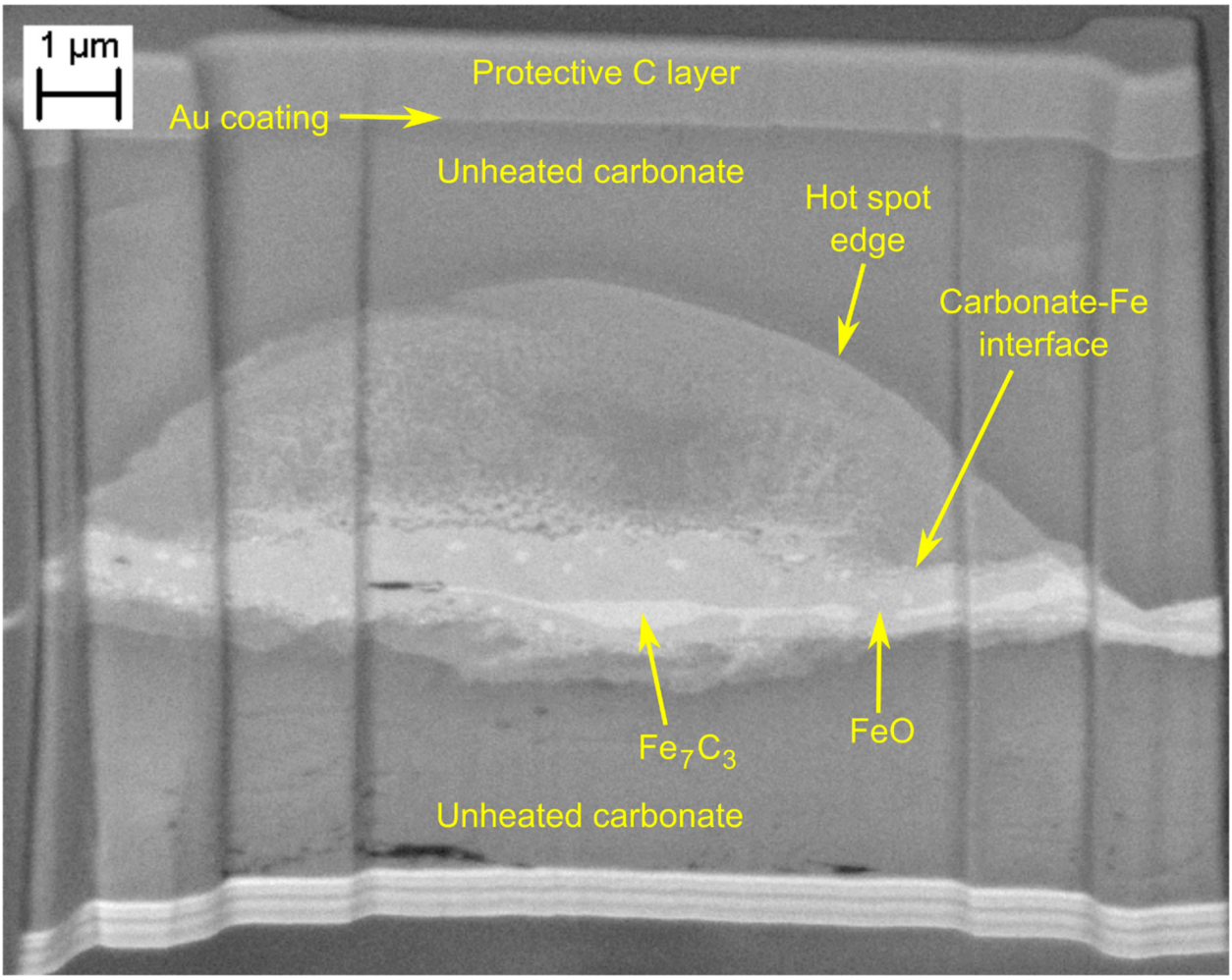

507

508 Figure 1: Backscattered scanning electron image recorded at 4 kV of dolomite-iron reaction
509 interface in sample thin section recovered from 66 GPa and 1900-2200 K. The iron-rich region in
510 the center appears brightest due to its high density. The extent of iron diffusion into and reaction
511 with the Fe-poor carbonate is also evident based on density. A few micron offset in alignment of
512 upstream and downstream lasers may be responsible for asymmetry of heated spot.

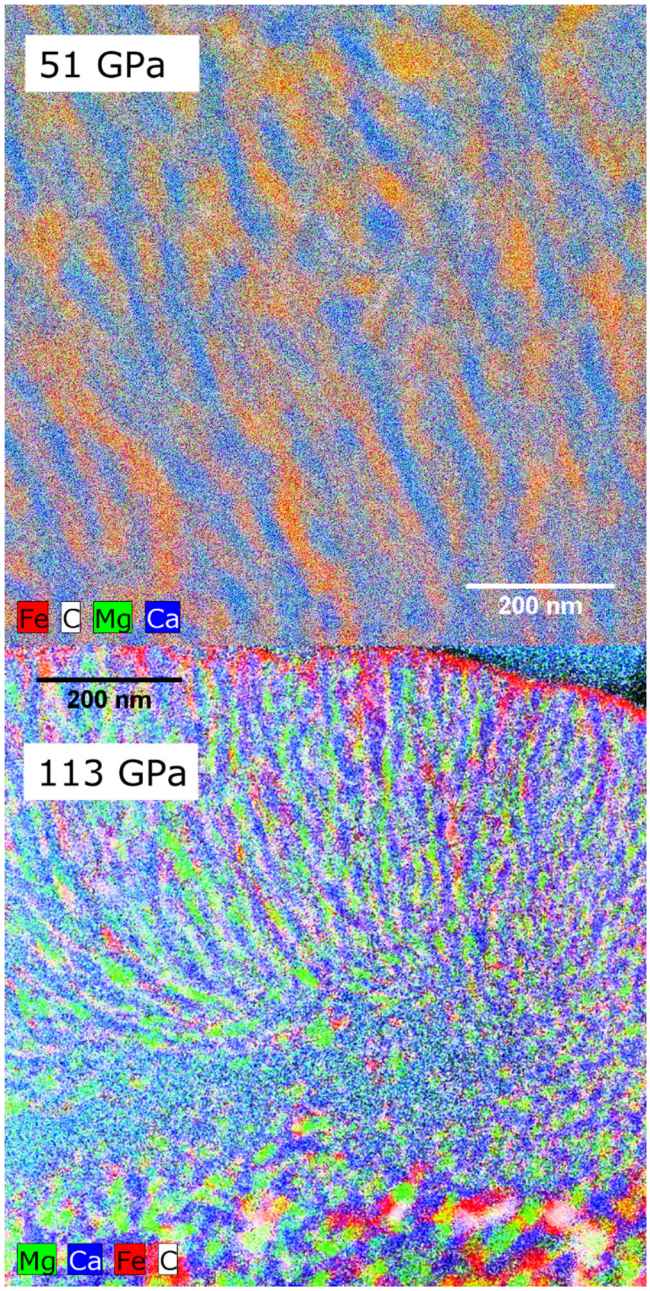

Figure 2: Energy-dispersive X-ray image of a) exsolution of two carbonates from dolomite at 51 GPa and b) formation of Fp + C + $CaCO_3$ at 113 GPa. Elements color-coded as follows: red=iron, blue=calcium, green=magnesium, white=carbon.

518 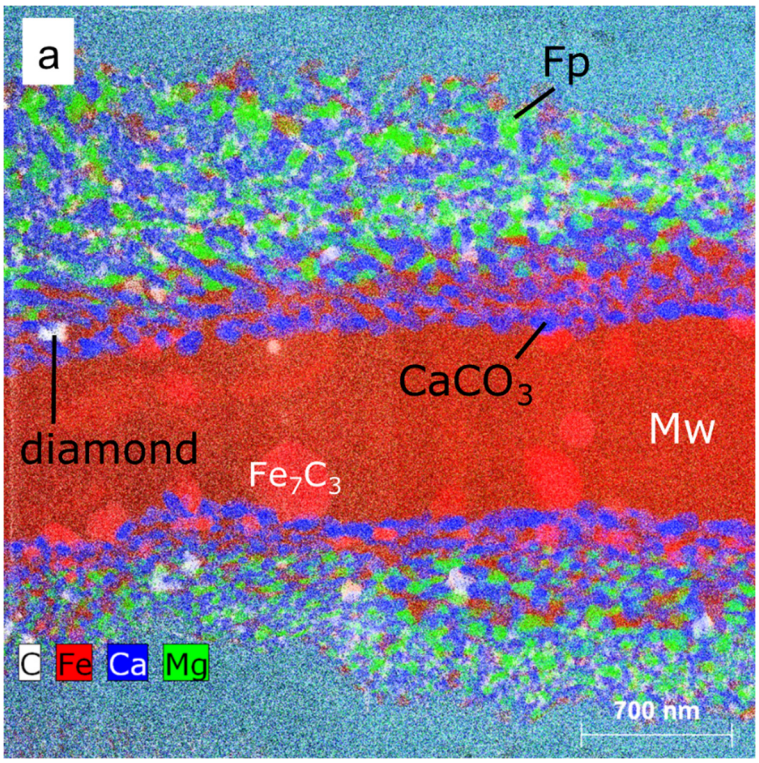

519 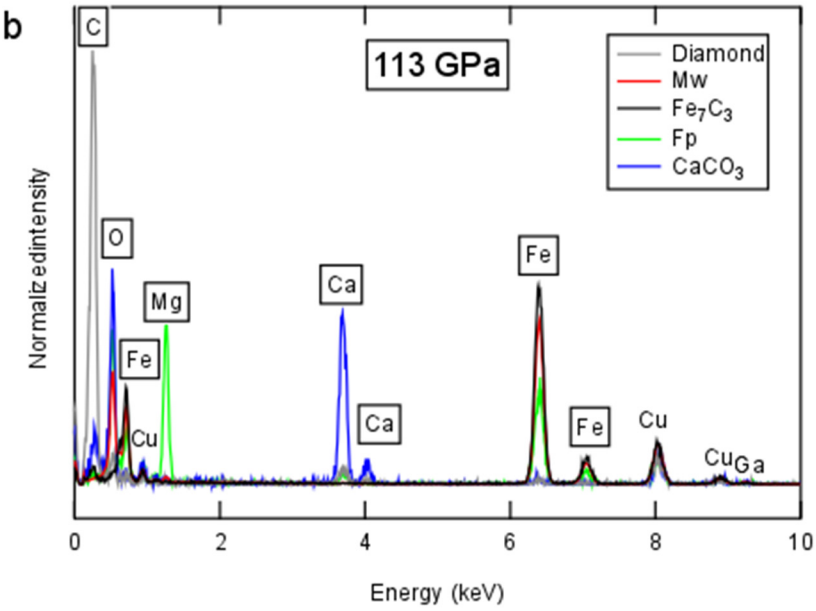

520 Figure 3: Composition measurements for dolomite-iron sample recovered from 113 GPa and

521 2400-2500 K. a) Energy-dispersive X-ray map with elements color-coded as follows: red=iron,

blue=calcium, green=magnesium, white=carbon. b) Examples of EDX spectra obtained for each phase.

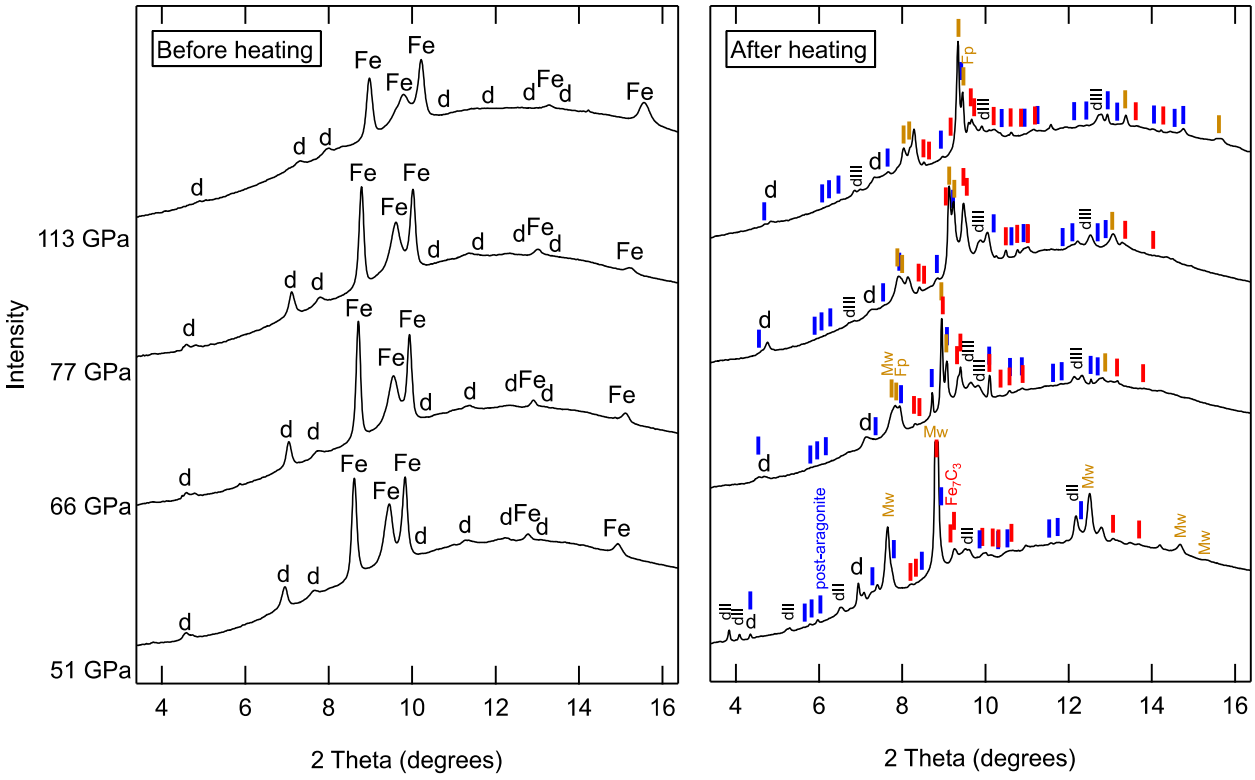

524

525 Figure 4: X-ray diffraction patterns observed before and after transforming samples of dolomite
526 (d) and iron foil (Fe) to magnesiowüstite and ferropericlase (gold Mw and Fp), Fe_7C_3 (red), and
527 post-aragonite-type $CaCO_3$ (blue) at pressures 51-113 GPa and temperatures 1800-2500 K in the

laser-heated diamond anvil cell. Additional diffraction peaks from high-pressure polymorphs of dolomite are labelled dII and dIII. For these experiments λ=0.3100 Å.

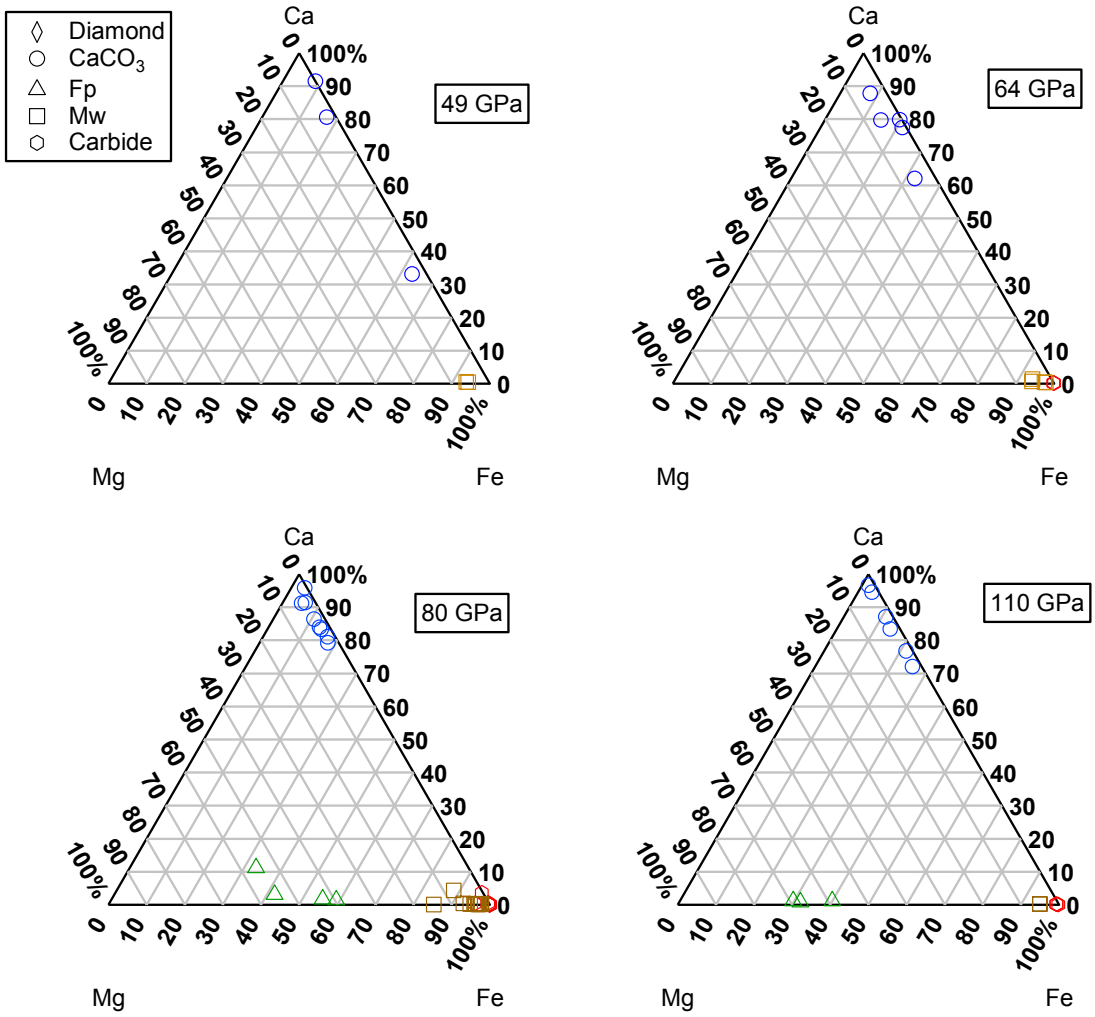

Figure 5: Compositions for observed phases obtained from EDX spectra plotted on Mg-Fe-Ca ternary diagrams.

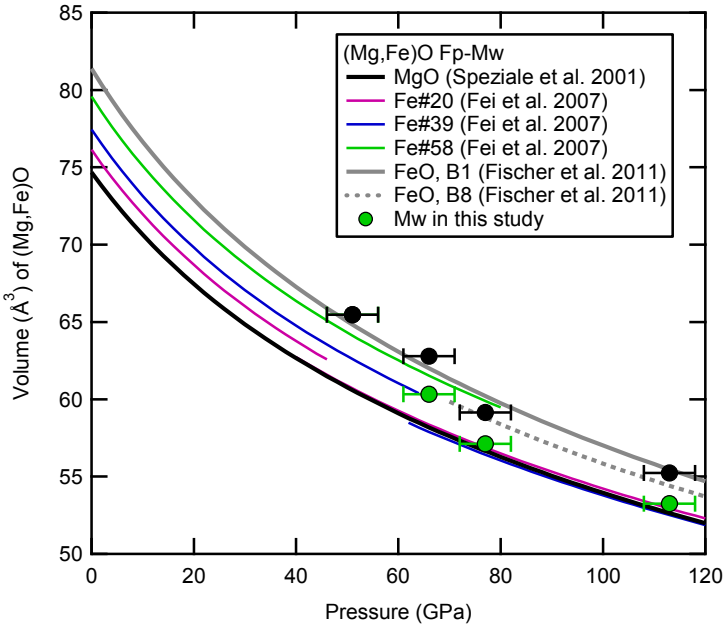

Figure 6: Observed unit cell volumes for Mw (black) and Fp (green) in this study plotted relative to previously-measured equations of state for Fp-Mw compositions with different Fe#=Fe/(Mg+Fe) (Fei et al., 2007; Fischer et al., 2011; Speziale et al., 2001). Pressures for data in this study are assumed to be the same as pressures obtained from the Fe foil before heating. (Mg,Fe)O diffraction peaks are split, indicating unit cell volumes consistent with coexistence of FeO at the sample center and ~$(Mg_{0.6}Fe_{0.4})O$ produced by breakdown of the dolomite. A decrease in unit cell volume observed in both oxides between 66 and 77 GPa is consistent with the spin transition in iron-rich Mw and structural change in FeO under these conditions.

545 Table 1.

546 Pressure, temperature, and heating duration for all experiments. Pressures given were obtained
547 before heating from the equation of state of the iron foil (Mao et al., 1990). Temperature
548 differences between downstream and upstream sides were typically observed to be ~100 K and
549 varied by ~100 K over the heating duration.

Pressure before heating (GPa)	Temperature (K)	Duration (min)
51	1800-2050	15
66	1900-2200	10
77	1900-2200	20
113	2400-2500	10

550
551